

Load transfer between cross-linked walls of a carbon nanotubeAlexandre F. Fonseca,^{1,*} Tammie Borders,^{2,†} Ray H. Baughman,^{3,‡} and Kyeongjae Cho^{1,4,§}¹*Department of Materials Science and Engineering, The University of Texas at Dallas, Richardson, Texas 75080, USA*²*Department of Chemistry, University of North Texas, Denton, Texas 76203, USA*³*The Alan G. MacDiarmid NanoTech Institute and the Department of Chemistry, The University of Texas at Dallas, Richardson, Texas 75080, USA*⁴*Department of Physics, The University of Texas at Dallas, Richardson, Texas 75080, USA*

(Received 26 August 2009; revised manuscript received 17 December 2009; published 28 January 2010)

Cross links between inner and outer walls of multiwalled carbon nanotubes are believed to increase nanotube modulus and therefore nanotube effectiveness for reinforcing composites. In order to investigate changes in the Young's modulus of individual double-walled nanotubes (DWNTs) as a function of cross-link density and type, molecular-dynamics simulations are employed to evaluate strain coupling and corresponding load transfer from outer to inner walls. Results show that interwall sp^3 bonds and interstitial carbon atoms can increase load transfer between DWNT walls and that interwall sp^3 bonds are most effective. However, the maximum size of the modulus increase is limited to about 25% for the investigated small-diameter, short DWNTs because the defects decrease the stiffnesses of the nanotube walls.

DOI: [10.1103/PhysRevB.81.045429](https://doi.org/10.1103/PhysRevB.81.045429)

PACS number(s): 62.25.-g, 81.07.De, 81.05.Qk, 31.15.xv

I. INTRODUCTION

Carbon nanotubes (CNTs) are considered to be the ultimate mechanical fillers for reinforcement of polymer composites.¹⁻³ The combination of small size, low density, large aspect ratio, and very high mechanical, electronic, and thermal properties that are achievable for individual carbon nanotubes makes them attractive candidates for composites for diverse applications.³⁻⁵

The mechanical properties of many different types of CNT-polymer composites have been studied both experimentally⁶ and theoretically.^{4,7} However, many of the different methods used for producing these composites have not provided major mechanical properties improvement, regardless the type and volume fraction of the CNTs used for reinforcement.^{3,4} Examples are certain CNT-epoxy composites^{2,8} and CNT-plastic composites that are melt processed.³

While the reasons for not achieving high mechanical properties can be related to the lack of efficient polymer-CNT interfacial stress transfer or poor dispersion of CNTs within the polymer matrix,^{3,9} it has been proposed^{2,10} that cross links between inner and outer walls of multiwalled carbon nanotubes (MWNTs) would increase CNT-polymer composite mechanical properties for instances where these former problems are solved. The low force constant for shear between the walls of MWNTs (Refs. 11–15) provides a limitation on MWNT use as reinforcing agents, since tensile strains on outer walls are little transferred to inner walls unless the MWNTs are very long. The use of cross links is proposed to help correct this problem.

Motivated by experimental studies demonstrating that electron,¹⁶⁻¹⁹ ion,²⁰ or neutron²¹ irradiation methods induce the appearance of defects and cross links between layers in graphite or between inner and outer walls of MWNTs, molecular-dynamics (MD) simulations have been used to study the load transfer behavior of MWNTs having different cross-link structures under different load conditions. Xia and

Curtin²² studied the dependence of inner wall pullout force and friction for a double-wall nanotube (DWNT) on the type of inner wall end termination. Xia *et al.*²³ investigated the transverse shear, uniaxial compression, and pullout loading in DWNTs with interwall sp^3 bonds. Huhtala *et al.*¹⁰ calculated the forces needed to start the sliding of the inner wall in DWNTs having different defect types. Peng *et al.*¹⁹ performed MD simulations to study the load transfer in DWNTs with Frenkel-pair²⁴-like defects. Shen *et al.*²⁵ studied load transfer between inner and outer walls of DWNTs under tensile and compressive loads, compared the results for capped and uncapped nanotubes, and studied one case where the defects are interstitial carbon atoms. HaiYang and XinWei²⁶ studied the mechanical properties of DWNTs having a regular pattern of sp^3 bonds between their walls. Very recently, Byrne *et al.*²⁷ showed that MWNTs with interwall sp^3 bonding are stronger than single-wall nanotubes (SWNTs) with the same number of intrawall defects. All of this work demonstrated significant improvement in load transfer between nanotube walls as a result of cross linking.

While pullout and sliding forces are important when fracture of the inner or outer wall takes place, previous work has not systematically studied how interwall bridging influences the load transfer before CNT rupture. In this paper, we investigated how tensile strain is transferred from outer to inner walls of DWNTs for different densities of two different types of cross-linking defects, namely, *interstitial carbon* and *direct interwall sp^3 bonding* between the walls (called “IC” and “SP³” for short, respectively). The choice of these two types of defects was made based not only on previous theoretical work but also on recent experimental results showing the possibility of having MWNTs with either type of defect. Urita *et al.*¹⁷ reported the observation of interstitial-vacancy pair defects in DWNTs at temperatures below 400 K. Kanasaki *et al.*²⁸ showed that femtosecond laser excitation is able to create metastable sp^3 -bonded carbons between layers of graphite. In a very recent theoretical paper, Muniz *et al.*²⁹ demonstrated the stability of sp^3 bonding between the layers of MWNTs. It is important to note that the interstitial car-

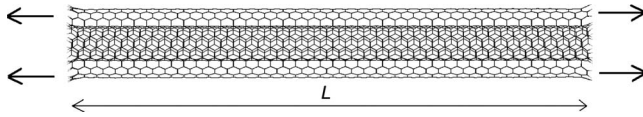


FIG. 1. Scheme of load transfer between inner and outer walls of a DWNT of length L . Arrows on both sides of the DWNT indicate the resultant tensile forces felt by the outer wall due to the interfacial stresses from a surrounding stretched matrix (matrix not drawn).

bons in IC defects also form sp^3 bonds with adjacent atoms. However, we kept the SP^3 name for the second defect since the walls are directly connected via a sp^3 bond rather than through an additional atom. While other types of defects can also be formed,^{10,24,30} IC and SP^3 defects represent the two main possibilities.

We will show that both types of defects significantly improve load transfer between the walls of the DWNTs, with the *interwall* SP^3 the more efficient type of cross link. We verify that if the defects substantially deform the nanotube hexagon structure, nanotube stiffness decreases. We complete the analysis by taking a perfect DWNT and randomly adding hydrogen atoms to the external side of the outer wall to simulate the effects of the pyramidalization^{31,32} of the corresponding outer wall carbons due to functionalization or chemical bonding between a polymeric matrix and the DWNT. In this case, the stiffness of the DWNT slightly decreases with increase in the number of these bonds. Furthermore, for the interwall defects, we will analyze the variation of the Young's modulus based on a simple mechanical model for the load transfer between the walls of a DWNT.

This paper is organized as follows. In Sec. II, we describe the systems, defect types, and molecular-dynamics (MD) methods employed in our study. In Sec. III, we describe the results and in Sec. IV we present our concluding remarks.

II. COMPUTATIONAL METHOD AND DESCRIPTION OF THE DWNT SYSTEMS

The reactive empirical bond order (REBO) potential, also named *Brenner-Tersoff* potential,^{33,34} is well known to accurately describe carbon-carbon and hydrocarbon interactions when allowing for bond breaking, recombination, and rehybridization. An extension to the second generation³⁴ of REBO to include pairwise van der Waals and torsional interactions, the so-called “adaptive intermolecular reactive empirical bond order” (AIREBO) (Ref. 35) potential will be employed to perform a MD study of load transfer between the walls of DWNTs.

The scheme of our study of load transfer from the outer to the inner wall of a DWNT is depicted in Fig. 1. An external strain is applied only to the outer wall and its effect on inner wall strain is measured.

Two DWNTs of different chiralities were chosen for the load transfer study: $(4,0)@(13,0)$ DWNT and $(5,5)@(10,10)$ DWNT, hereby called DWNT-1 and DWNT-2, respectively (where the first and second pairs of indices for each nanotube type describe the inner and outer nanotubes,

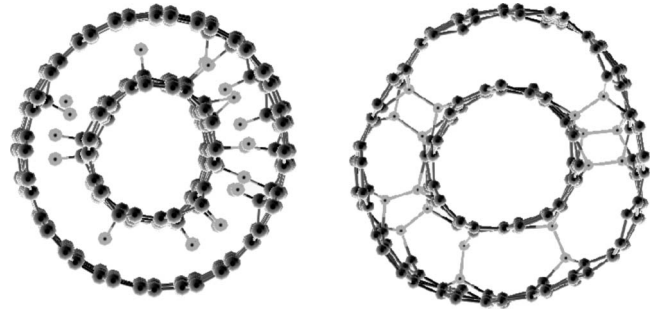


FIG. 2. Cross-sectional view of pieces of fully 0 K relaxed DWNT-2s with 50 cross links, showing examples of the local atomic structure of IC (left) and SP^3 (right) defects (light gray atoms), respectively.

respectively). These DWNTs satisfy the heat of formation stability rule $(m,0)@(m+9,0)$ and $(m,m)@(m+5,m+5)$ for zigzag and armchair tubes, respectively.³⁶ We passivated the nanotube ends with hydrogen and chose a total length $L \sim 100$ Å which gives ~ 1800 and ~ 2500 as the total number of atoms for DWNT-1 and DWNT-2, respectively. For every nanotube and for every type of defect, we studied five cases with different numbers of defects: 2, 25, 50, 75, and 100, plus the case with no defects for comparison. The defects were randomly distributed and in the cases of two defects, we chose samples where the defect positions were not close to each other, i.e., their distance was larger than half of total length of the nanotube. Using the definition of the *fraction of defects*, f , as the number of cross-linking defects divided by the number of the atoms of the system,²³ the largest f considered in our work is smaller than 6% for the DWNT-1 with 100 SP^3 defects, a number similar to what was considered in Ref. 23. Figure 2 depicts examples of the local atomic structures of both IC and SP^3 defects for stress-free DWNT-2s equilibrated at 0 K.

After the initial 0 K relaxation of all structures, the tensile strain MD simulations were carried out as follows. First, the carbon atoms at the length-direction extremities of the outer wall were moved apart by 0.2 Å, corresponding to $\sim 0.2/100=0.2\%$ of tensile strain. Then, a new full 0 K relaxation of the structure was performed keeping only the carbon atoms at the extremities of the outer wall fixed. Atoms of the inner wall were always free to relax. Starting from this relaxed structure, the strain in the outer wall was increased to 0.4% by moving apart by an additional 0.2 Å the carbon atoms at the extremities of outer wall. Since we are interested in studying the elastic regime of deformation, this series of tensile strain simulations was performed up to a total maximum strain of $\sim 10\%$,^{37,38} resulting in 51 MD simulations for each DWNT, totaling 1122 simulations. Each relaxation was done for a total time of 100 ps (using a 0.5 fs of time step) in order to ensure full optimization of the structure. At each step, total energy and strains of inner and outer walls were collected in order to calculate the Young's modulus of the structure and the load transfer between the walls.

We also investigate load transfer between inner and outer walls of DWNTs for the case where a fraction of the carbons in the outer shell are derivitized (so that they become sp^3 carbon). It was hoped that increased roughness of the outer

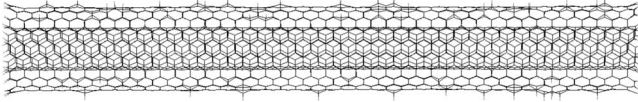


FIG. 3. Lateral view of the DWNT-2 with 100 hydrogens on the outer wall. The hydrogen-bonded carbons display their pyramidalization. Carbon and hydrogen atoms are drawn in black and gray, respectively.

shell would increase load transfer to the inner wall of the DWNT. The system evaluated is depicted in Fig. 3 which is composed of a DWNT with a specified number of hydrogen atoms randomly bonded to its outer wall carbon atoms, thus producing the so-called *pyramidalization*^{31,32} of the carbon due to the addition of a fourth bond (making these carbon atoms become sp^3). We, then, performed tensile strain MD simulations, as previously described, to study the load transfer between the outer and inner walls of the DWNT. Analogously to the defect cases described above, we considered five different numbers of nanotube-hydrogens bonds on the surface of the DWNT: 2, 25, 50, 75, and 100. These MD tensile strain simulations were carried out only for DWNT-2 and for a total maximum strain of $\sim 1\%$.

In order to study the stiffness of the nanotube, we used the following expression:⁴

$$Y = \frac{1}{V} \frac{\partial^2 E}{\partial \epsilon^2}, \quad (1)$$

where E is the strain energy, ϵ the tensile strain, and $V=LA$ is the volume of the nanotube, where L is the total length and $A=2\pi Rh$ is the cross-sectional area of the nanotube, with R

being its cross-section radius and $h=0.34$ nm the wall thickness as usually considered in theoretical and experimental studies of carbon nanotube Young's modulus.⁴ Equation (1) is the usual definition of the Young's modulus of a tube, but in our case we considered only the outer wall cross-sectional area since the external stresses were applied only to the outer wall. Therefore, we call it *effective Young's modulus*. Including both walls, the DWNTs will decrease this modulus of DWNT-1 and DWNT-2 by factors of 0.765 and 0.667, respectively. If the area of the central void cylinder is also considered (as it must be for most practical purposes other than evaluation of density normalized modulus), this reduction of the single-wall modulus of DWNT-1 and DWNT-2 further increases to factors of 0.751 and 0.641, respectively.

III. RESULTS AND DISCUSSION

We analyzed load transfer from outer to inner walls of both DWNT-1 and DWNT-2 by inspecting the inner wall strain variation as a function of the applied outer wall tensile strain. Figure 4 shows these variations hereafter called *outer-to-inner load transfer strain curves*. The first and second rows of Fig. 4 show the results for DWNT-1 and DWNT-2, respectively. The first and second columns show results for IC and SP^3 defects, respectively.

While both SP^3 and IC cross-link types provide major increase in the load transfer between the walls of the DWNTs, relative to that for perfect DWNTs, we can clearly see in Fig. 4 that the degree of stress transfer of the SP^3 defect is about twice that of the IC defects. The reason for this difference can be understood in terms of mobility of the defects and the energetic costs of deformations. The migra-

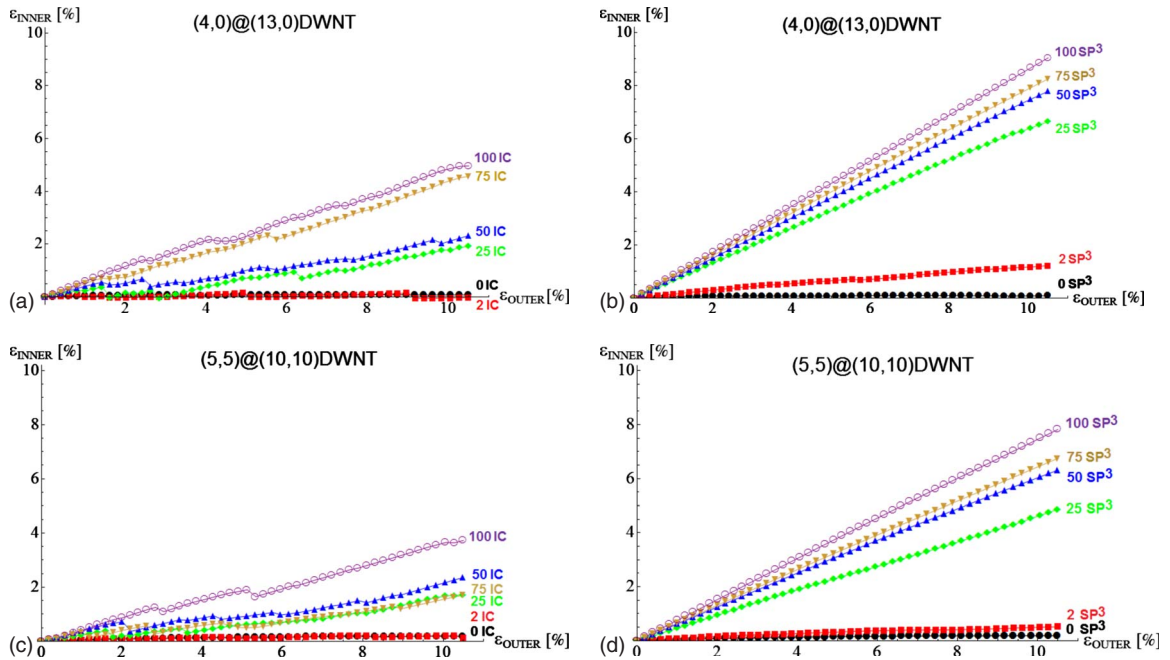


FIG. 4. (Color online) Strain of inner wall, ϵ_{INNER} , as a function of strain applied to the outer wall, ϵ_{OUTER} , for (4,0)@(13,0) DWNT (first row) and (5,5)@(10,10) DWNT (second row). The first and second columns show the results for the IC and SP^3 defects, respectively. The curves are for 100 defects (magenta open circles), 75 (light brown triangle-down), 50 (blue triangle-up), 25 (green diamond), 2 (red square), and no defects (filled circles) in the 100 Å nanotubes. Symbols are MD simulation results and lines are guides for the eyes.

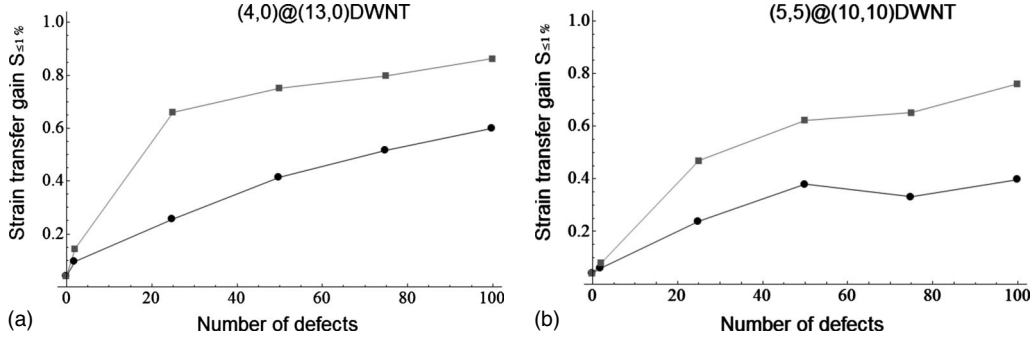


FIG. 5. Strain transfer gain curves at $\bar{\epsilon} \leq 1\%$ for (4,0)@(13,0) DWNTs (left) and (5,5)@(10,10) DWNTs (right) for different numbers of IC (black circles) and SP^3 (gray squares) defects. Symbols are MD simulation results and lines are guides for the eyes.

tion energy barrier of individual interstitial carbon atoms in graphite is smaller than for other defect types.¹⁶ Hence, we expect that during application of strain to the outer nanotube wall, the energetic cost of moving the interstitial atoms to decrease stress transfer can become smaller than the cost of continuously increasing strains on the walls. Subsequent movement of the interstitial carbons is followed by contraction of the inner wall as a consequence of partial tensile strain energy release for the inner wall. We observe such strain releases (first column of Fig. 4) for the IC defect through discontinuities in inner wall strain as a function of applied outer wall strain, which are a consequence of movement of interstitial carbon atoms and partial release of strain energy for the inner wall.

In the case of direct sp^3 bonds between inner and outer walls, we cannot *a priori* determine whether the energetic cost of straining the hexagon structure of walls is larger than the cost of breaking the sp^3 -bond between them. However, the almost perfect linear behavior of the outer-to-inner load transfer strain curves, shown in the second column of Fig. 4, for SP^3 defects in DWNT-1 and DWNT-2, indicates that the cost of breaking the sp^3 bonds³⁹ is higher than the elastic strain applied to the walls, at least for strains up to the 10% exterior wall strain under quasistatic condition.

In order to compare the change in degree of strain transfer between outer and inner walls, for different numbers of defects, we define the parameter $S_{\bar{\epsilon}}$ (called strain transfer gain) as

$$S_{\bar{\epsilon}} \equiv \frac{d\epsilon_{\text{INNER}}}{d\epsilon_{\text{OUTER}}}, \quad (2)$$

where $\bar{\epsilon}$ is a given value of the outer wall strain up to which the slope is calculated and ϵ_{INNER} and ϵ_{OUTER} are the strains of inner and outer walls, respectively. Since strain transfer gain from outer to inner wall varies for the IC defects with the outer wall strain, we will compare the maximum gain by calculating $S_{\bar{\epsilon}}$ at low strains ($\bar{\epsilon} \leq 1\%$) just before the first abrupt variation. Figure 5 shows $S_{\bar{\epsilon} \leq 1\%}$ for both DWNTs with SP^3 and IC cross-link defects. In both cases, the slope increases with the number of defects and we verify that the load transfer from outer to inner walls is larger for the SP^3 defects than for the IC defects, even for small numbers of defects. Our data also show that the strain transfer gain converges to a value between 0.4 and 0.6 for the IC defect and between 0.6 and 0.9 for the SP^3 defect.

Figure 6 shows the effective Young's moduli of the DWNTs for both types of defects as a function of the number of defects on the 100 Å long nanotube. Effective Young's moduli were calculated using Eq. (1) and the MD data for outer wall strains up to 1%. Figure 6 shows that the effective Young's modulus of the DWNTs increases with the number of defects at least in some defect concentration ranges, with the SP^3 defects the more effective for strain transfer. In order to understand these results, a simple mechanical model is proposed as follows. If the DWNT has no cross links, an external force applied to the outer wall will cause, in the

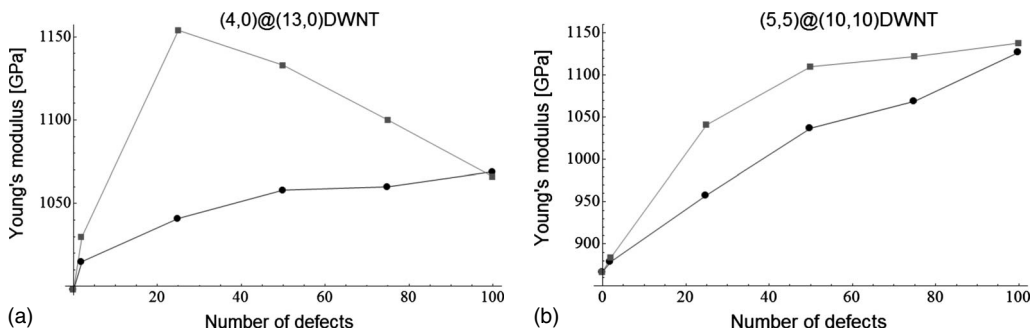


FIG. 6. Effective Young's moduli of (4,0)@(13,0) DWNTs (left) and (5,5)@(10,10) DWNTs (right) for different numbers of IC (black circles) and SP^3 (gray squares) defects. Symbols are MD simulation results and lines are guides for the eyes.

linear elastic regime, a strain inversely proportional to its stiffness. As the number of cross links increases, the external force is divided among the outer and inner walls, thus producing respective outer and inner strains also in accordance to their stiffnesses. If F is the resultant external force acting on the outer wall of the DWNT, we can write

$$F = F_1 + F_2, \quad (3)$$

where F_1 and F_2 are the net forces acting separately on outer and inner walls, respectively. If ΔX_1 and ΔX_2 are the axial displacements due to the action of forces F_1 and F_2 , the resultant force is simply given by

$$F = k_1 \Delta X_1 + k_2 \Delta X_2, \quad (4)$$

where k_1 and k_2 are the stiffnesses of the outer and inner walls, respectively. Now, using the definition of strain transfer gain, ($S_{\bar{\epsilon}}$), given in Eq. (2), we can write $\Delta X_2 = S_{\bar{\epsilon}} \Delta X_1$, which when substituted in Eq. (4) gives

$$F = (k_1 + S_{\bar{\epsilon}} k_2) \Delta X_1. \quad (5)$$

If the dependences of k_1 and k_2 on defect concentration were negligible, the maximum effective Young's modulus would be obtained for the maximum value of $S_{\bar{\epsilon}}$ (which is for $S_{\bar{\epsilon}}=1$, when inner and outer walls can be considered to behave as a parallel association of equally strained springs¹⁹). However, in general, k_1 , k_2 , and $S_{\bar{\epsilon}}$ in Eq. (5) will depend on the type and number of defects. The limited increase of modulus (Fig. 6) as a consequence of defect incorporation (compared to the ~ 1 TPa modulus of graphite and the nearly identical modulus for the defect-free outer wall of the DWNTs) is a consequence of decreases of inner and outer wall force constants as a result of defect incorporation. This effect is most clearly seen in the effective Young's moduli of (4,0)@(13,0) DWNTs that contain SP^3 defects (Fig. 6), where the modulus reaches a maximum value at about 25 defects per 100 Å DWNT length and then decreases with further increase in defect concentration (while $S_{\bar{\epsilon}}$ increases monotonically with defect concentration as shown in Fig. 5).

To test this assumption of decreased stiffness of the individual walls of DWNT-1 with increasing defect concentration, we performed another sequence of MD tensile strain simulations as a function of SP^3 defect number for DWNT-1, but in this case both inner and outer walls were equally stretched. In this case, Eq. (1) calculated effective Young's modulus of the DWNT takes into account the full van der Waals cross-section area of the nanotube (rather than just the van der Waals cross section of the outer nanotube as for the other calculations). The left side of Fig. 7 shows that this area-corrected Young's modulus of DWNT-1 decreases with increasing number of SP^3 defects, when complete coupling between strain in neighboring walls is artificially imposed. This verifies that the decrease of DWNT-1 stiffness in Fig. 6 occurs due to structural changes in the nanotube walls.

In order to identify which structural changes are causing the decrease in the DWNT-1 stiffness, we have inspected the inner and outer wall atomic structures of DWNT-1 as a function of the number of sp^3 bonds. We found out that the inner wall atomic structures are dramatically changed by SP^3 defects. Because the inner wall of (4,0) nanotube is small, sp^3

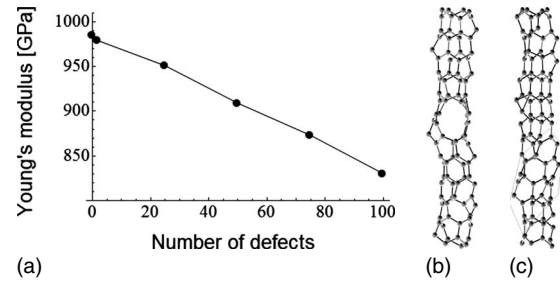


FIG. 7. (Left) Area corrected Young's moduli of (4,0)@(13,0) DWNTs for different numbers of SP^3 defects calculated by applying equal tensile strain to both inner and outer walls. Symbols are MD simulation results and lines are guides for the eyes. (Middle) Part of the structure of the inner wall of the DWNT-1 with 100 SP^3 defects showing a hole. (Right) Same as shown in the middle but rotated to show a groove (region inside the thin gray lines).

bonds to the outer wall can cause holes and grooves in the inner wall structure, as shown in Fig. 7 (middle and right panels). These holes and grooves cause a decrease in stiffness of the DWNT-1 with the increase of the number of sp^3 bonds. Interstitial carbons do not generate similar deformations as can be seen (Fig. 2) in the almost regular cross-sectional shapes of DWNT-1 containing IC defects.

The decrease in wall modulus with increase in number of cross links is exaggerated by the small diameter of the inner walls of the presently evaluated DWNTs. The introduction of the same number of cross links per unit nanotube length between adjacent walls is expected to have a smaller effect on nanotube structure (and likely wall stiffness) for larger diameter DWNTs. Also, MWNTs have a more highly confined structure, which will likely limit structural changes due to cross linking and the achievable extent of this cross linking.

In the case of formation of IC defects by irradiation, generation of vacancies in the walls of irradiated nanotubes is expected. Because vacancies cannot directly cause interwall load transfer, other than potentially by increasing surface roughness, we have not considered the effect of vacancies in our study of load transfer. Addition of vacancies will decrease the modulus of nanotube walls, both by decreasing the number of covalent bonds in the walls and distorting the wall structure.⁴⁰ Similar to the effects of vacancies on the stiffness of bundles of SWNTs with intertube cross links,⁴¹ there will be an interplay between the increase of the effective Young's modulus due to the presence of IC defects and wall modulus decrease due to the presence of vacancies. However, because it was also shown that the reduction of Young's modulus due to vacancies is less significant for nanotubes with large diameters,⁴⁰ the larger the diameter of a MWNT with IC defects, the smaller the contribution of vacancies in its outer walls to its effective Young's modulus. Inspecting the values of relative increase of the effective Young's modulus, with respect to the value for a perfect nanotube (see results for DWNT-1 and DWNT-2 in Fig. 6 left and right, respectively), the increase in effective Young's modulus is seen to increase with increasing nanotube diameter. Therefore, for large MWNTs with IC defects, the effect of vacancies on nanotube stiffness can be neglected compared to the effects of IC defects.

Results obtained on the effect of randomly adding hydrogen to the outer wall of the (5,5)@(10,10) DWNT are as follows. The resulting pyramidalization of the hydrogen-bonded carbons makes these carbon atoms move radially away from the inner wall. This may cause a decrease in interlayer stress transfer. Also, it is expected that the force constant for outer wall stress will decrease as a result of this derivitization of the outer DWNT wall. Whatever the explanation for this effect, the calculations show that randomly adding H substituents to the outer wall of this DWNT slightly decreases effective Young's modulus.

IV. CONCLUSION

Our MD quasistatic simulations show the effect of randomly located interwall cross links on interwall strain transfer and modulus for 100 Å long, small diameter DWNTs. Of the two types of cross links investigated, direct cross links (sp^3 defects) and cross links via interstitial carbon atoms (IC defects), the sp^3 defects provide the highest enhancement of interwall strain transfer and the highest enhancement of Young's modulus by associated force transfer (except at the highest observed defect concentration, where the Young's modulus is insensitive to defect type). Discontinuities in plots of inner wall strain versus outer wall strain are due to the energetic capability of the IC defects to relieve strain on the inner wall by shifting bonding site, which apparently does not occur for the sp^3 defects, where there are no discontinuities in the linear relationship between applied outer wall strain and resulting inner wall strain up to the maximum applied outer wall strain of 10%.

Additional details are as follows. Transfer of a strain on the external DWNT wall to the inner wall is close to complete for 100 sp^3 defects on a 100 Å long DWNTs containing 1800–2500 total carbons and still large, but reduced, when the defect concentration is halved (Fig. 4). The transfer of outer wall strain to inner wall strain is sharply decreased (by an amount that depends on defect concentration) when sp^3 cross-linking defects are replaced by the same number of IC defects. Similar results were obtained for (4,0)@(13,0) and (5,5)@(10,10) DWNTs containing the same type and concentration cross-linking defect, though stress transfer from outer to inner wall was greatest for the former DWNT (Fig. 4).

A maximum effective Young's modulus increase (of about 25%) on defect incorporation was achieved for incorporation of either sp^3 defects or IC defects in (5,5)@(10,10) DWNTs. However, the maximum observed effective Young's modulus had similar values for both nanotubes and both defect types. Computationally observed degradation of wall stretching force constants due to wall structure limits the increase of effective Young's modulus due to interwall cross links. For the investigated DWNT having the smaller initial inner wall diameter [(4,0)@(13,0) DWNT], effective Young's modulus reached a maximum, at about 25 sp^3 defects per 100 Å tube length and then sharply decreased for higher defect concentrations, while for the IC defect in the (4,0)@(13,0) DWNT or either defect in the (5,5)@(10,10) DWNT, the maximum effective Young's modulus was for the highest defect con-

centration. This result suggests that degradation of wall stiffness is largest for sp^3 defects in the (4,0)@(13,0) DWNT, which is reasonable considering the small inner wall diameter.

We have not modified the cutoff distance to at least partially correct the overestimation of the maximum force needed to break a carbon-carbon bond.⁴² The reason is that we are concerned with the linear elastic regime of the deformations of the DWNTs and the study of the dependence of nanotubes elastic properties on cross-linking type and density in a situation resembling the composite.

Although the Ref. 28 reported the formation and metastability of sp^3 bonded carbons in graphite by femtosecond laser excitation, the stability of our sp^3 defects presented by AIREBO potential should be further investigated. Since Frenkel pair defects also are formed by sp^3 bonds, our results, at small temperatures and strains, would be similar if the cross-linking type is the Frenkel pair. *Ab initio* and DFT calculations are going to be employed in future investigations of the stability of these defects in different carbon nanotubes.

We have seen (Fig. 4) that for the largest numbers of sp^3 defects, the inner wall strain nearly follows the strain applied to the outer wall. Therefore, we expect that when the outer wall strain reaches its failure strain value, inner wall strain will be also close to its failure strain value. In the case of an external strain causing the breaking of the outer wall, the inner walls linked to the outer one by sp^3 bonds would also break. This was experimentally observed by Peng *et al.*¹⁹ They showed that the number of broken most-external walls of MWNTs subjected to large tensile strains was just 1 for the nonirradiated MWNTs (so without any cross link) and more than 1 for all electron irradiated MWNTs. This indicates that load transfer is very efficient for defect induced MWNTs as predicted by our simulations.

Less extensive studies were conducted on the effect of outer wall derivitization by random hydrogen substitution on interwall strain transfer. These results are for (5,5)@(10,10) DWNT, a maximum number of hydrogen substitutions of 100 for the 100 Å long DWNT, and a maximum strain of 1%. We found that this hydrogen substitution slightly decreases DWNT effective Young's modulus. The resulting pyramidalization of the hydrogen-bonded carbons makes these carbon atoms move radially away from the inner wall. This may cause a decrease in interlayer stress transfer. Also, such derivitization can potentially decrease shell stiffness. Whatever the explanation for this effect, the calculations show that the overall effect was slight degradation of the effective Young's modulus for the investigated DWNT.

ACKNOWLEDGMENTS

This work was partially supported by Lockheed Martin. A.F.F. acknowledges partial support from the Brazilian agency CNPq. R.H.B. acknowledges support from NSF Grant No. DMI-0609115 and Robert A. Welsh Foundation Grant No. AT-0029.

- *afonseca@puvr.uff.br. Present address: Pólo Universitário de Volta Redonda, Universidade Federal Fluminense, Av. dos Trabalhadores 420, Volta Redonda, RJ, Brazil, CEP:27255-125.
- †tammie.l.borders@lmco.com
- ‡ray.baughman@utdallas.edu
- §kjcho@utdallas.edu
- ¹R. H. Baughman, A. A. Zakhidov, and W. A. de Heer, *Science* **297**, 787 (2002).
 - ²L. S. Schadler, S. C. Giannaris, and P. M. Ajayan, *Appl. Phys. Lett.* **73**, 3842 (1998).
 - ³J. N. Coleman, U. Khan, and Y. K. Gun'ko, *Adv. Mater.* **18**, 689 (2006).
 - ⁴D. Srivastava, C. Wei, and K. Cho, *Appl. Mech. Rev.* **56**, 215 (2003).
 - ⁵B. I. Yakobson, C. J. Brabec, and J. Bernholc, *Phys. Rev. Lett.* **76**, 2511 (1996).
 - ⁶See Ref. 3 and references therein.
 - ⁷C. Wei, D. Srivastava, and K. Cho, *Nano Lett.* **2**, 647 (2002).
 - ⁸P. M. Ajayan, L. S. Schadler, C. Giannaris, and A. Rubio, *Adv. Mater.* **12**, 750 (2000).
 - ⁹W. Ma, L. Liu, Z. Zhang, R. Yang, G. Liu, T. Zhang, X. An, X. Yi, Y. Ren, Z. Niu, J. Li, H. Dong, W. Zhou, P. M. Ajayan, and S. Xie, *Nano Lett.* **9**, 2855 (2009).
 - ¹⁰M. Huhtala, A. V. Krasheninnikov, J. Aittoniemi, S. J. Stuart, K. Nordlund, and K. Kaski, *Phys. Rev. B* **70**, 045404 (2004).
 - ¹¹J. Cumings and A. Zettl, *Science* **289**, 602 (2000).
 - ¹²B. H. Hong, J. P. Small, M. S. Purewal, A. Mullokandov, M. Y. Sfeir, F. Wang, J. Y. Lee, T. F. Heinz, L. E. Brus, P. Kim, and K. S. Kim, *Proc. Natl. Acad. Sci. U.S.A.* **102**, 14155 (2005).
 - ¹³A. Kis, K. Jensen, S. Aloni, W. Mickelson, and A. Zettl, *Phys. Rev. Lett.* **97**, 025501 (2006).
 - ¹⁴M.-F. Yu, B. I. Yakobson, and R. S. Ruoff, *J. Phys. Chem. B* **104**, 8764 (2000).
 - ¹⁵S. B. Legoas, V. R. Coluci, S. F. Braga, P. Z. Coura, S. O. Dantas, and D. S. Galvão, *Phys. Rev. Lett.* **90**, 055504 (2003).
 - ¹⁶F. Banhart, *Rep. Prog. Phys.* **62**, 1181 (1999).
 - ¹⁷K. Urita, K. Suenaga, T. Sugai, H. Shinohara, and S. Iijima, *Phys. Rev. Lett.* **94**, 155502 (2005).
 - ¹⁸A. V. Krasheninnikov and F. Banhart, *Nature Mater.* **6**, 723 (2007).
 - ¹⁹B. Peng, M. Locascio, P. Zapol, S. Li, S. L. Mielke, G. C. Schatz, and H. D. Espinosa, *Nat. Nanotechnol.* **3**, 626 (2008).
 - ²⁰B. Ni, R. Andrews, D. Jacques, D. Qian, M. B. J. Wijesundara, Y. Choi, L. Hanley, and S. B. Sinnott, *J. Phys. Chem. B* **105**, 12719 (2001).
 - ²¹J. Seldin and C. W. Nezbeda, *J. Appl. Phys.* **41**, 3389 (1970).
 - ²²Z. Xia and W. A. Curtin, *Phys. Rev. B* **69**, 233408 (2004).
 - ²³Z. H. Xia, P. R. Guduru, and W. A. Curtin, *Phys. Rev. Lett.* **98**, 245501 (2007).
 - ²⁴R. H. Telling, C. P. Ewels, A. A. El-Barbary, and M. I. Heggie, *Nature Mater.* **2**, 333 (2003).
 - ²⁵G. A. Shen, S. Namilae, and N. Chandra, *Mater. Sci. Eng., A* **429**, 66 (2006).
 - ²⁶S. HaiYang and Z. XinWei, *Physica B* **403**, 3798 (2008).
 - ²⁷E. M. Byrne, M. A. McCarthy, Z. Xia, and W. A. Curtin, *Phys. Rev. Lett.* **103**, 045502 (2009).
 - ²⁸J. Kanasaki, E. Inami, K. Tanimura, H. Ohnishi, and K. Nasu, *Phys. Rev. Lett.* **102**, 087402 (2009).
 - ²⁹A. R. Muniz, T. Singh, E. S. Aydil, and D. Maroudas, *Phys. Rev. B* **80**, 144105 (2009).
 - ³⁰Another reason for considering the SP^3 defect is that we have performed a comparative study between the Frenkel pair and the SP^3 defect type in DWNTs and observed that the Frenkel pair is less stable than the SP^3 . We also have done some high-temperature molecular-dynamics simulations that show that Frenkel pair defects evolve to SP^3 ones.
 - ³¹S. Park, D. Srivastava, and K. Cho, *Nanotechnology* **12**, 245 (2001).
 - ³²S. Park, D. Srivastava, and K. Cho, *Nano Lett.* **3**, 1273 (2003).
 - ³³D. W. Brenner, *Phys. Rev. B* **42**, 9458 (1990).
 - ³⁴D. W. Brenner, O. A. Shenderova, J. A. Harrison, S. J. Stuart, B. Ni, and S. B. Sinnott, *J. Phys.: Condens. Matter* **14**, 783 (2002).
 - ³⁵S. J. Stuart, A. B. Tutein, and J. A. Harrison, *J. Chem. Phys.* **112**, 6472 (2000).
 - ³⁶B. Shan and K. Cho, *Phys. Rev. B* **73**, 081401(R) (2006).
 - ³⁷C. Wei, K. Cho, and D. Srivastava, *Phys. Rev. B* **67**, 115407 (2003).
 - ³⁸C. Wei, K. Cho, and D. Srivastava, *Appl. Phys. Lett.* **82**, 2512 (2003).
 - ³⁹Our estimates of the energy barrier to break the sp^3 bond between the inner and outer walls and recover the perfect DWNT, using the AIREBO potential, is ~ 1 eV per sp^3 bond. This value is similar to the corresponding energy barrier for a Frenkel pair defect in two layers of graphene, ~ 1.4 eV (see Ref. 24).
 - ⁴⁰M. Sammalkorpi, A. Krasheninnikov, A. Kuronen, K. Nordlund, and K. Kaski, *Phys. Rev. B* **70**, 245416 (2004).
 - ⁴¹M. Sammalkorpi, A. V. Krasheninnikov, A. Kuronen, K. Nordlund, and K. Kaski, *Nucl. Instrum. Methods Phys. Res. B* **228**, 142 (2005).
 - ⁴²O. A. Shenderova, D. W. Brenner, A. Omeltchenko, X. Su, and L. H. Yang, *Phys. Rev. B* **61**, 3877 (2000).